ACS OMEGA

http://pubs.acs.org/journal/acsodf

Article

Impedimetric Sensors for Cyclocreatine Phosphate Determination in Plasma Based on Electropolymerized Poly(*o*-phenylenediamine) Molecularly Imprinted Polymers

Ibrahim F. Abo-Elmagd, Amr M. Mahmoud,* Medhat A. Al-Ghobashy, Marianne Nebsen, Nesrine S. El Sayed, Shahira Nofal, Sameh H. Soror, Robert Todd, and Salwa A. Elgebaly

Cite This: *ACS Omega* 2021, 6, 31282−31291

Read Online

ACCESS | Metrics & More | Article Recommendations | Supporting Information

ABSTRACT: Cyclocreatine and its water-soluble derivative, cyclocreatine phosphate (CCrP), are potent cardioprotective drugs. Based on recent animal studies, CCrP, FDA-awarded Orphan Drug Designation, has a promising role in increasing the success rate of patients undergoing heart transplantation surgery by preserving donor hearts during transportation and improving the recovery of transplanted hearts in recipient patients. In addition, CCrP is under investigation as a promising treatment for creatine transporter deficiency, an X-linked inborn error resulting in a poor quality of life for both the patients and the caregiver. A newly designed molecularly imprinted polymer (MIP) material was fabricated by the anodic electropolymerization of *o*-phenylenediamine on screen-printed carbon electrodes and was successfully applied as an impedimetric sensor for CCrP determination to dramatically reduce the analysis time during both the clinical trial phases and drug development process. To enhance the overall performance of the proposed sensor, studies were performed to optimize the electropolymerization conditions, incubation time, and pH of the background electrolyte. Scanning electron microscopy, electrochemical impedance spectroscopy, and cyclic voltammetry were used to characterize the behavior of the developed ultrathin MIP membrane. The CCrP-imprinted polymer has a high recognition affinity for the template molecule because of the formation of 3D complementary cavities within the polymer. The developed MIP impedimetric sensor had good linearity, repeatability, reproducibility, and stability within the linear concentration range of 1×10^{-9} to 1×10^{-7} mol/L, with a low limit of detection down to 2.47×10^{-10} mol/L. To verify the applicability of the proposed sensor, it was used to quantify CCrP in spiked plasma samples.

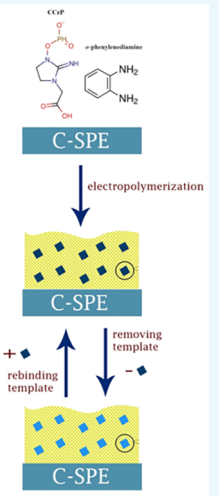

1. INTRODUCTION

Cyclocreatine phosphate (CCrP) is a water-soluble derivative of cyclocreatine (CCr) that is used clinically to preserve donor hearts and improve the recovery of the transplanted hearts in recipient patients during heart transplantation surgery.[1−3] The Food and Drug Administration (FDA) has awarded the Orphan Drug Designation (ODD) status for CCrP in the process of "Prevention of Ischemic Injury to Enhance Cardiac Graft Recovery and Survival in Heart Transplantation".[1,2] In addition, CCrP is under investigation as a promising treatment for creatine transporter deficiency (CTD), an X-linked inborn error resulting in a poor quality of life for both the patients and the caregiver. Unfortunately, there are no current available therapies for CTD. This increases the needs for fast, cost-effective methods for determining CCrP in patient serum, dietary supplements, and rodent serum.

Due to the crucial role that CCrP plays, we inspected the analytical methodologies used for its monitoring closely.[4,5] CCrP detection is difficult to analyze using conventional high-performance liquid chromatography (HPLC) as it is a highly polar molecule that is nonelectroactive and nonfluorescent and has a weak UV absorption signal. Moreover, the presence of structural analogue compounds in biological fluids at high concentration, such as creatine (Cr), CCr, creatine phosphate (CrP), and adenosine triphosphate (ATP) makes the task even more challenging. A literature survey revealed that CCrP has only reported to be monitored with methods based on hydrophilic interaction liquid chromatography (HILIC), which can analyze highly hydrophilic small molecules.[4,5] From the analytical chemistry standpoint, HPLC is considered the benchmark standard for pharmaceutical analysis; however, it has various limitations related to its high cost, long cycle time, and high organic solvent consumption.[6,7] Alternatively, impedimetric sensors have numerous advantages such as low energy usage, ability to detect nonelectroactive molecules, high sensitivity, relatively simple, and eco-friendly process. Furthermore, such sensors can be highly selective based on modifying the electrode surface with suitable surface

Received: September 14, 2021
Accepted: October 27, 2021
Published: November 11, 2021

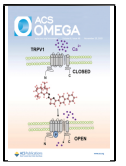

recognition elements, such as antibodies, aptamers, or molecularly imprinted polymers (MIPs).[8−10] Therefore, establishing a sensor based upon MIP for CCrP measurement provides a promising and advantageous alternative to determine small polar molecules in plasma. This could reduce the analysis time dramatically during both clinical trial phases and the drug development process.

Sensors are considered an interesting area for research as they are highly useful in multidisciplinary fields, such as environmental monitoring, food production, bioprocess control, health care, and biotechnology.[11−13] Most sensors are based on a recognition element that is able to recognize a specific target molecule and subsequent transduction of the recognition into an output signal.[14,15] Designing materials that have good recognition properties compared with biological receptors is difficult in many cases.[16] MIP materials are considered a powerful and remarkable synthesis platform for producing polymer-type artificial receptors.[17−20] This process involves the construction of a host molecule via a polymerization process with a target guest molecule as a template in the polymerization matrix. Then, the embedded template is removed, and "imprint sites" are formed in the remaining matrix to facilitate the recognition of molecules that are closely related to the structure of the template molecule.[21] One molecular imprinting strategy involves the use of noncovalent imprinting, which does not limit the choice of analysis methods.[22] Noncovalent imprinting offers high selectivity, even for small molecules with no functionality.[23] The imprinting process involves polymerization of functional monomers in the presence of a template molecule (target molecule). Removing the template produces a recognition site for a complementary molecule with appropriate 3D size, and chemical functionality is provided to facilitate selective binding to the target.[9] Molecularly imprinted electrochemical sensors are a type of MIP that synergistically combines the advantages of MIP (in particular their selectivity) with those of electrochemical sensors, such as high sensitivity, simple operation, portability, low cost, user friendliness, and fast analysis.[24,25] The molecular imprinted electrochemical sensors based on graphene,[26] nanocomposites,[27] carbon nanotubes,[26] and carbon nitride nanotubes[28,29] have been intensely used for analysis in last years. In terms of research over the past few years, efforts have been focused on the development of molecularly imprinted electrochemical sensors based on the synthesis of polymers with a predetermined selectivity for a particular target substance.[30]

Electropolymerization has been reported as an excellent method for preparing MIPs through in situ polymerization of the monomers at an electrode surface, as it offers a simple way to generate homogeneous binding sites for the target template.[30,31] In comparison with other polymerization methods, electropolymerization has many advantages:[9,32] (1) it does not require free radical initiators, oxidants, or light to initiate polymerization; (2) it can be performed at room temperature; (3) the polymer forms adherent, dense, uniform, and conformal ultrathin films on the electrode surface; (4) the film thickness can be precisely controlled and reproduced by controlling the electrochemical conditions (voltage, current, number of cycles, and polymerization time); and (5) polymerization and operation in aqueous media is possible.[31,33,34] Selection of the functional monomers has received much attention due to its critical role in targeting a template molecule and its relation to the medium conditions. Moreover, it defines the shape and characteristics of the template molecule in the aqueous solution.[31] To the best of our knowledge, there is no previous study focused on developing an electrochemical sensor based on electropolymerization for the determination of CCrP.

Aniline and its derivatives are considered a promising class of compounds in the field of molecular imprinting.[35] For example, *ortho*-phenylenediamine (*o*-phenylenediamine; *o*-PD) is a diamine compound that is structurally related to aniline and has been used as a monomer for the synthesis of various MIP compounds.[36] Upon oxidation, *o*-PD forms a polymeric matrix of poly-*o*-PD (P*o*PD), where the chemical and physical features of P*o*PD are highly dependent on the reaction conditions, such as the oxidation method and pH.[37] P*o*PD has attracted much interest as a substrate to be functionalized in the MIP field.[37−39] It is used as a preparative strategy to identify surfaces with specific functionality.[40,41] There are many candidates for the electrosynthesis of MIP reported in the literature[42] such as pyrrole, *oo*-PD, thiophene, phenol, and recently dopamine, and levodopa. In this respect, spectroscopic studies (such as UV−Vis and NMR) of the monomer−analyte complex can shed light on the system to be polymerized. In our study, the monomer showed high affinity toward our template as indicated spectroscopically, which motivated us to fabricate the sensor using *o*-PD as the candidate monomer.

In the current study, a MIP membrane for CCrP detection was developed (to the best of our knowledge, for the first time) by electropolymerization of *o*-PD onto carbon screen-printed electrodes (C-SPEs) with a CCrP template. Electrochemical impedance spectroscopy (EIS) was used for sensor signal transduction; the sensor process fabrication is electropolymerized using *o*-PD. To fabricate a sensor, an ultrathin membrane with excellent insulation characteristics is crucial for performance optimization. Thus, cyclic voltammetry (CV) was used to obtain electrically insulting thin films on modified electrodes through electropolymerization of *o*-PD. Electrochemical characterization using CV and EIS was performed to ensure the modification of the CCrP-imprinted membrane on the SPE surface. CCrP sensor characterization and calibration curves were established and fully validated. Finally, the proposed sensor was used for CCrP measurements of spiked plasma samples.

2. RESULTS AND DISCUSSION

The noncovalent imprinting process was introduced by the Mosbach group[43] and is based on noncovalent interactions between specific functional groups on the polymerizable monomers and template. This method has been widely used to fabricate highly sensitive and selective sensors.[44,45] Since 1990,[43] noncovalent MIPs have proven to be highly selective, and they can even differentiate between compounds that differ only by the presence of a methyl group,[21] and differentiate between enantiomers. Hence, they have been used in many fields, including separation science and electrochemistry.[46−48]

2.1. Sensor Fabrication by Electropolymerization of *o*-PD. Previously, *o*-PD has been electropolymerized on several substrate materials.[49] Figure 1 shows the CV results during the electropolymerization of *o*-PD at pH 7.0 using 20 cyclic scans in the presence of a CCrP template; the results of the control experiment where CCrP is absent are shown in Figure S1. There are two changes: first one is the disappearance of this peak at 0.3 V, which is probably due to formation of a complex between the monomer and the template. Second one is shifting

https://doi.org/10.1021/acsomega.1c05098
ACS Omega 2021, 6, 31282−31291

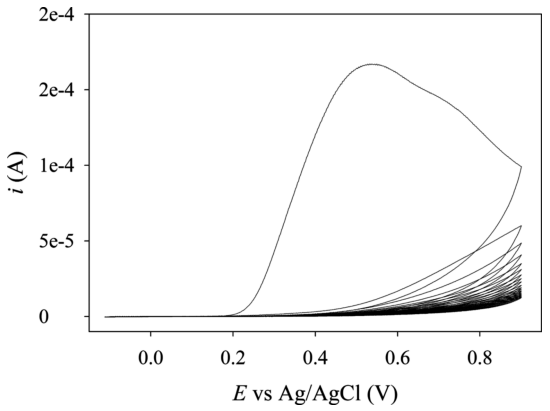

Figure 1. Cyclic voltammograms for the electropolymerization of *o*-PD at C-SPE/MIP (0.01 M *o*-PD, 0.01 M CCrP).

the start of the oxidation potential of the *o*-PD template complex to the left compared to the *o*-PD solution alone. Electrochemistry is a very sensitive method, and it can be used to determine the complexation constant based on the shift of the redox potential. During the first cycle, the *o*-PD oxidation current was high and oxidation started at 0.2 V. Subsequently, the peak current declined dramatically with every successive scan until the current flow was highly diminished in the cell. The voltammetric behavior of *o*-PD indicates an irreversible oxidation process, resulting in the formation of bonds on the electrode surface. These results indicate that a self-limiting, nonconducting, ultrathin film that is adherent to the electrode surface was formed during electropolymerization scans. The insulating polymer was able to block electron transfer between the *o*-PD monomers and the electrode/solution interface. These results are in agreement with the previous literature.[35,50]

2.2. Physical and Electrochemical Properties of the MIP. *2.2.1. Morphology.* The morphology and thickness of the C-SPE/MIP samples were examined at high magnifications using scanning electron microscopy (SEM) (Figure 2). The surface and plane morphology of the polymer film indicated that it was well dispersed and homogeneous (Figure 2A−C), suggesting that it had a sufficiently high surface coverage to adsorb CCrP. Additionally, the cross section revealed a layered structure with a thickness of 3.11−5.51 μm (Figure 2D−F), and the membrane appeared porous, while SEM image of C-SPE/NIP shows the formation of an adherent smooth film on the top of the carbon electrode (Figure S2). The porosity of the MIP film will not only increase its surface area but also facilitate the CCrP diffusion into the exposed 3D cavities within the MIP membrane porous structure which will greatly enhance the sensor response time.

2.2.2. Electrochemical Properties. EIS was performed to characterize the C-SPE/MIP electrodes as it is an efficient method for analyzing interfacial phenomena.[51] Here, impedance measurements were performed to assess the electrode charge-transfer resistance (R_{CT}) and double layer capacitance (C_{DL}) behavior. Fitting of the data for the C-SPE/MIP electrode was performed using Randles' equivalent circuit (Figure S3). Figure 3 shows Nyquist plots of the C-SPE/MIP before and after the washing step. The initial R_{CT}, which is a directive and sensitive parameter that responds to changes in the electrode−solution interface, was high for this membrane. After washing the electrode with water for 30 min, its R_{CT} decreased significantly, indicating that CCrP was removed from the MIP cavities and accessible imprinted sites were formed. This conclusion is supported by comparing these results with those for C-SPE/NIP, where no significant difference in the Nyquist plots was observed under similar experimental conditions after washing (Figure S4).

It should be noted that template removal is a critical step as it has a tangible effect on the sensitivity and reproducibility of the sensors. This step can be performed by solvent extraction or electrochemical methods. The common solvent extraction technique for template removal from MIP films is performed using organic reagents or buffer solutions as eluents. However, the use of ultrapure water has been reported frequently in the literature, especially for removing hydrosoluble molecular templates (such as ascorbic acid, sorbitol, and glucose) from MIPs.[50,52,53] One study compared the use of ultrapure water to that of two frequently used solvents (10% aqueous acetic acid and absolute alcohol) to remove an ascorbic acid template by immersing ascorbic acid−PoPD/C-SPE samples in one of the three solvents for 20 min.[53] It was found that both acetic acid and absolute alcohol changed the microstructure of the PoPD film, which contributed to nonspecific adsorption. Therefore, ultrapure water was used in this study to remove the embedded template.

Furthermore, CV experiments were used to ensure the successful synthesis of the CCrP-MIP on the electrode surface (Figure 4). Using the bare SPE as a control, $[Fe[CN]_6]/[Fe[CN]_6]^{3-/4-}$ showed a pair of reversible redox peaks. Coating of the electrode surface with P*o*PD polymer resulted in a reduction in the intensity of these peaks for both C-SPE/NIP and C-SPE/MIP. These results indicate that a nonconducting adherent MIP membrane was formed on the electrode surface that was able to block the redox peak of $[Fe[CN]_6]/[Fe[CN]_6]^{3-/4-}$. Thus, an electrode with good insulating properties was successfully developed, which was then verified for impedimetric CCrP determination.

2.2.3. Binding and Molecular Recognition of CCrP by C-SPE/MIP. The noncovalent polymerization method has few constraints on the choice of template, where a prepolymerization complex needs to be formed between the functional monomers and the template based on typical attraction forces, such as hydrogen bonding. Thus, *o*-PD is a suitable functional monomer for producing MIPs, as it provides hydrophobic, hydrophilic, and basic recognition sites through electrostatic interactions[54] that may enable the formation of a stable adduct with the template. The driving force of the recognition process is probably related to interactions between the rigid structure of the imprinted cavities and the template.

In the imprinted membrane, CCrP is encapsulated within imprinted cavities and is adsorbed via interactions between the monomer and the template. To investigate such interactions, Figure S5 shows spectroscopy results for CCrP, *o*-PD, and an equimolar sample of *o*-PD and CCrP. Both an increase in the intensity and shift of the *o*-PD peak were observed, providing evidence for the mentioned interaction. These interactions expected to be related to hydrogen bonding or van der Waals binding forces, such as the formation of multiple hydrogen bonds between the negative phosphate group, P═O bond of template molecules, and (−NH−) and ($-NH_2$) groups in the polymer structure. Multiple hydrogen bonds between the CCrP phosphate group and PoPD polymer play a critical role in sensor selectivity, as discussed later.

By examining the structure of our target analyte, CCrP is capable of forming multiple hydrogen bonds with *o*-PD monomers because carboxylic, phosphate, and nitrogen groups

https://doi.org/10.1021/acsomega.1c05098
ACS Omega 2021, 6, 31282−31291

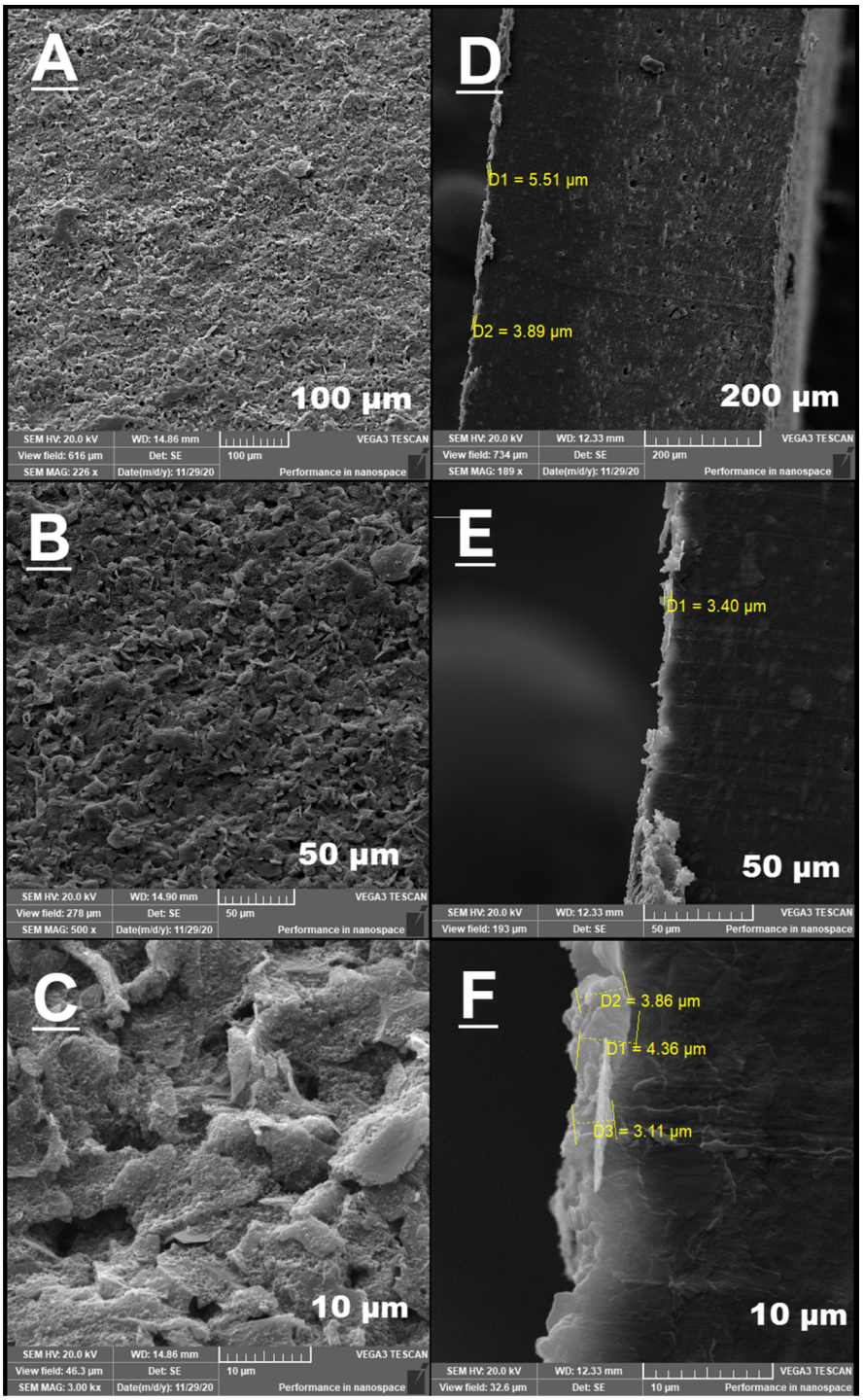

Figure 2. SEM images of C-SPE/MIP: top view (A−C) and its cross section (D−F).

are all able to form hydrogen bonds with the polymer backbone. It is well known in biochemistry that phosphate group "phosphorylation" can form multiple hydrogen bonds with amino acids, and by the addition of phosphate groups to proteins, kinase enzymes may be capable of mediating post-translational modifications.[49,55] Therefore, imprinting selective 3D cavities that are specific to template recognition has been performed successfully in aqueous solutions, where many hydrogen bonds occur between the analyte and template prepolymerization complex. However, electrostatic interactions cannot be completely excluded as previous studies highlighted that electrostatic forces may be present, even in a neutral medium. This can explain the inconsistencies between previous computational and experimental results, where electrostatic forces play a significant role in addition to hydrogen bonds in the interaction between *o*-PD and the template.[21]

2.3. Optimization of Experimental Conditions. In the current study, the conditions used in the electropolymerization process for preparing the MIP were optimized, namely, the number of scan cycles, incubation time, and pH.

2.3.1. Number of Cycles. The polymer thickness can be easily controlled and reproduced by optimizing the voltage,

https://doi.org/10.1021/acsomega.1c05098
ACS Omega 2021, 6, 31282−31291

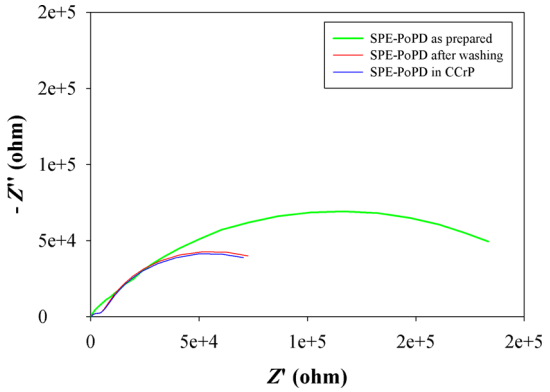

Figure 3. Nyquist plot of the C-SPE/MIP as prepared (green) and before (blue) and after (red) washing.

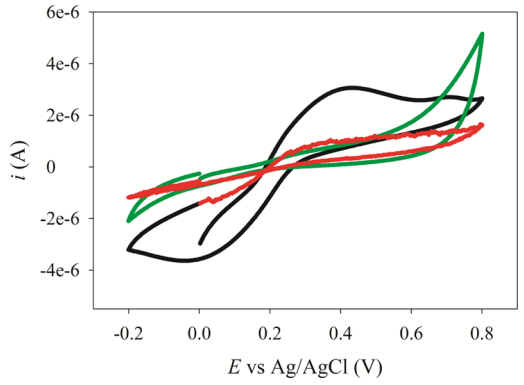

Figure 4. Voltammograms of SPE in the presence of $[Fe[CN]_6]/[Fe[CN]_6]^{3-/4-}$ redox couple, black line: bare electrode; green Line: C-SPE/NIP; red line: C-SPE/MIP.

number of cycles, or current during the electropolymerization process. The electrode surface of an impedimetric sensor must provide sufficient electrical insulation.[56] Initially, four scan cycles were selected according to the literature,[39,50] but it was noted that the polymer films formed on the C-SPE surface had superior sensor performance when a high number of scan cycles (20) was used. This improvement in sensor performance was attributed to the formation of an ultrathin insulating film that efficiently incorporates the template during electropolymerization and improves the behavior of the developed MIP membrane.

2.3.2. Incubation Time and pH of Background Electrolyte. As the diffusion of the CCrP template into the MIP is not instantaneous, the optimal incubation time of the sensor immersed in the sample was investigated by measuring the sensor response at 5 min intervals over 5−25 min. The measured capacitance values increased over time and plateaued after 15 min. Therefore, the MIP sensor should be incubated in the analyte solution for a 15 min "accumulation time" prior to measurement, presumably due to slow diffusion and binding kinetics.[9]

To select an appropriate pH of the background electrolyte for the proposed sensor, different pH values were determined within the pH range of 2−10. Borate buffer with pH 8.5 showed the maximum sensitivity and was thus considered the optimal pH. The optimal activity of the sensor as a function of pH was determined based on the negatively charged CCrP, which is thought to be incorporated into the P*o*PD film via multiple hydrogen bonds that stabilize the molecule within the 3D imprinted cavities.[57] At pH 8.5, the P*o*PD backbone will be neutral as the *o*-PD monomer has $pK_{a1} < 2$ (+2) and $pK_{a2} = 4.47$ (+1). However, it should be stressed again that multiple hydrogen bonds are capable of providing sufficient interaction between the target analyte and polymer backbone. Our experimental results are consistent with a recent report for detecting anionic perfluorooctanesulfonate using P*o*PD,[58] where the authors reported an optimal detection pH of 8.4 (similar to our optimal pH of 8.5). They argued that this pH was optimal because the anionic group is bound to a relatively small hydrophobic backbone. These findings were considered while selecting the optimal conditions for our impedimetric measurements.

2.4. Determination of CCrP in Biological Fluids. Under the optimal conditions in borate buffer (pH 8.5) and after 15 min of incubation time at the electrode surface, a CCrP calibration curve was produced using spiked plasma. There was a linear relationship between the charge-transfer capacitance of the MIP membrane and the CCrP concentration in the range of 1×10^{-9} to 1×10^{-7} M ($R^2 = 0.996$). It should be noted that C-SPE/NIP showed minimum response "As shown in Figure S4, the NIP capacitance change upon exposure to challenging concentration; 10^{-5} M CCrP was about 46.2 nF, while for MIP upon exposure to similar concentration capacitance change was over 278.4 nF" to the CCrP solution, indicating the importance of the 3D cavities in the MIP in the recognition process and the subsequent generation of the signal.

2.5. Bioanalytical Method Validation. Validation of the developed method assessed according to the FDA guidelines resulted in metrics within the acceptable limits.

2.5.1. Linearity, LOD, and LOQ. Figure 5 shows the calibration curve of the CCrP in spiked plasma. LOD and

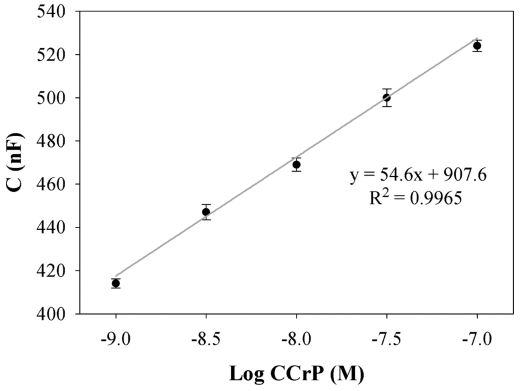

Figure 5. Calibration curve of capacitance vs logarithmic concentration of CCrP in spiked plasma sample ranges of 1×10^{-9} to 1×10^{-7} M.

LOQ were 2.47×10^{-10} and 8.25×10^{-10} mol/L, respectively. As a result, it is clear from comparing the proposed method with the published ones for CCrP determination that our method provides a linearity range (22.9−0.23 ng/mL) close to those of reported tandem mass spectroscopy methods.[4,5] Figure S6 provides the EIS experiment result with different CCrP concentrations.

2.5.2. Selectivity. To assess the selectivity of the developed MIP capacitive sensor toward CCrP, the interference of structural analogue molecules (Cr, CCr, CrP, and ATP) was investigated, where their chemical structures are shown in

https://doi.org/10.1021/acsomega.1c05098
ACS Omega 2021, 6, 31282−31291

Figure S7. The concentration of the structural analogues was selected based on their estimated concentration in the real biological samples.[4] Figure 6 indicates that the selectivity of the

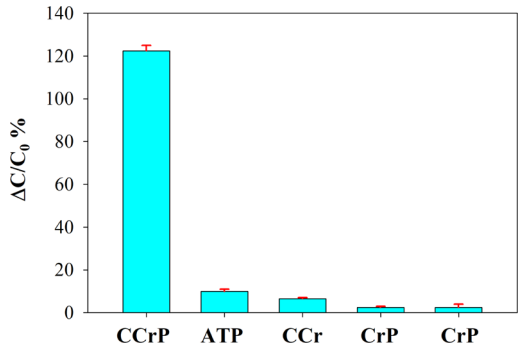

Figure 6. Relative capacitance change of the MIP capacitive sensor for 10^{-8} CCrP and other interferences at 10^{-5} concentration at the same CCrP-imprinted polymer film.

MIP capacitive sensor is closely associated with the type of functional group, molecular structure (shape and size), and charge of the interfering species. The selectivity of the developed imprinted sensor was evaluated by assessing its response to some potential interferences. In the experiments, Cr, CCr, CrP, and ATP were used to investigate its selectivity.

Figure 6 shows the change in C_{DL} of the developed MIP membranes upon interaction with 10^{-8} M CCrP and various interfering molecules (ATP, CCr, CrP, and Cr) over 15 min. In the case of the C-SPE/MIP CCrP sensor, an apparent capacitance change was observed for ATP (8.2%) and CCr (5.3%), while only minimal capacitance changes (<2.0%) were observed for Cr and CrP, even at a high concentration (10.0 μM).

The surprising low selectivity of the C-SPE/MIP sensor toward CCr (the parent drug of CCrP) reflects the importance of the multiple hydrogen bonding interactions between P*o*PD and the phosphate moiety in CCrP, which greatly enhance the binding toward CCrP compared to CCr. Moreover, the same argument explains the high interference of ATP compared to CrP; although both have phosphate groups, ATP has three phosphate groups, while CrP has only one. Therefore, ATP shows the highest interference with the MIP sensor through formation of hydrogen bonds with P*o*PD. In addition, ATP is expected to be the most strongly bound peripheral to the P*o*PD surface by multiple hydrogen bonds and therefore produces the highest observed interference. This explains why CrP has a higher interference than Cr. These results confirm that the C-SPE/MIP sensor has good selectivity for CCrP recognition in biological fluids. These results are consistent with previous reports. Electropolymerized MIP sensors have been reported as excellent selective sensors for their target templates in the presence of structural analogues, such as targeting glucose in the presence of fructose,[50] sorbitol in the presence of glycerol,[52] caffeine in the presence of theophylline (differing only by a methyl group),[59] and even the enantiomeric selectivity for L-glutamate in the presence of D-glutamate.[60]

2.5.3. Accuracy and Precision. Spiked plasma at the three QC levels (QCL, QCM, and QCH) was prepared and analyzed to test the within run and between run accuracy and precision on 3 consecutive days. The CCrP sensor had an intraday accuracy of 100.33% with a precision of 0.57% and an interday accuracy of 100.38% with a precision of 0.82%. All results are listed in Table S1.

2.5.4. Recovery and Matrix Effect. Plasma protein precipitation using methanol/water (1:1) has proven to be a successful and simple way to prepare plasma samples with good recovery. Assessment of the matrix effect (ME) is considered a cornerstone for assay validation. In this study, either suppression or enhancement effects were measured by comparing the capacitance according to eq 1 [ME (%) = Set 2 (Matrix)/Set 1 (Neat solvent) × 100], as described previously. The results summarized in Table 1 show matrix enhancement across the studied QC levels for CCrP (173.53 ± 1.74%). In contrast, the process efficiency (PE) calculated from eq 3 [PE % = Set 3 (Plasma)/Set 1 (Neat solvent) × 100%] takes into consideration both the recovery and ME. Therefore, recovery efficiency (RE) was calculated from eq 2 [Set 3 (Plasma)/Set 2 (Matrix) × 100%], which provides the actual recovery of the analyte (108.02% ± 1.83) not affected by ME, while PE (187.49 ± 3.54%) describes the efficiency of the overall process.

The large ME is common for capacitive sensors and dominated by the ionic strength of the sample.[61] Another factor that can contribute to the ME is the use of methanol during protein precipitation. It is worth noting that the RSD is considered low, which ensures the validity and linearity of the data. Because EIS is a sensitive surface technique, the initial background is sensitive to the surroundings. This is a major advantage for monitoring cell cultures and bacterial growth just by monitoring changes in the growth medium. Therefore, changes in the capacitance (and/or resistance) are monitored and frequently reported in the literature. Thus, the calibration for each matrix should be performed separately before the measurement.

2.5.5. Stability. The prepared quality-control samples were subjected to three freeze−thaw cycles. The resulting mean

Table 1. Recovery and Matrix Effect for the Determination of CCrP

	ME (%)[a]	RE (%)[b]	PE (%)[c]	freeze and thaw cycle (%)	bench top stability (%)
QCH	176.30	110.08	194.07	98.39	96.78
QCM	174.00	107.82	187.60	97.56	96.32
QCL	170.31	106.15	180.79	97.31	97.65
mean ± RSD	**173.53 ± 1.74**	**108.02 ± 1.83**	**187.4 ± 3.54**	**97.75 ± 0.71**	**96.92 ± 1.06**

[a]ME expressed as the ratio of the capacitance of an analyte fortified post extraction (Set 2, Matrix matched) to the capacitance of the same analyte standards (Set 1, Neat solvent) multiplied by 100. [b]RE calculated as the ratio of the capacitance of an analyte fortified before extraction (Set 3, Plasma) to the capacitance of an analyte fortified post extraction (Set 2, Matrix matched) multiplied by 100. [c]PE expressed as the ratio of the capacitance of an analyte fortified before extraction (Set 3, Plasma) to the capacitance of the same analyte standards (Set 1, Neat solvent) multiplied by 100.

https://doi.org/10.1021/acsomega.1c05098
ACS Omega 2021, 6, 31282−31291

recovery percentage of CCrP was in the range of 97.31−98.39% with a RSD of 0.58−0.85% (Table 1), which confirmed that repeated freeze−thaw cycles did not affect the quantification of the analyte. In addition, the prepared samples after extraction were left at room temperature for 6 h and then analyzed to study the bench-top stability; the mean recovery percentage of CCrP was in the range of 96.32−97.65% with a RSD of 0.51−1.71%. The results showed that there was no degradation of CCrP. In general, samples are considered stable if the results are within ±15% of the original concentration.[62] Moreover, the sensor showed good stability, as it was stored in a desiccator at room temperature for 1 month, and then, it was reused with no obvious change in the capacitance response.

3. CONCLUSIONS

A MIP membrane selective toward CCrP was successfully fabricated via electropolymerization of the *o*-PD monomer on a C-SPE substrate. The developed MIP offered satisfactory specificity and selectivity for the template molecule, even in the presence of the structural analogues abundant in biological fluids. Moreover, the proposed method could be easily extended to develop chemical sensors for other small molecules by selecting appropriate monomers in conjunction with a suitable transduction mechanism. EIS measurements may be a sensitive and convenient method for investigating MIPs, even with nonelectroactive embedded species. The developed impedimetric sensor provides a simple, accurate, precise, sensitive, and cost-effective approach to determine CCrP in sub-nanomolar concentrations in borate buffer at optimum pH. The sensor was highly effective for identifying CCrP in spiked human plasma at extremely low concentrations. To the best of our knowledge, this is the first study to identify CCrP with a practical method; existing studies have used HILIC UPLC−MS/MS analysis of rodent plasma, dietary supplement products, and CTD patient fibroblasts. Therefore, MIP membranes have great potential for use in faster and cost-effective CCrP detection.

4. EXPERIMENTAL SECTION

4.1. Instruments. A potentiostat/galvanostat PGSTAT204 (Metrohm Autolab, Netherlands) was used for electropolymerization of the MIP, along with CV and EIS measurements. A three-electrode configuration was used with the C-SPE as the working electrode (3 mm diameter; CH Instruments, Inc., TX, USA), Pt wire counter electrode, and Ag/AgCl (3 M KCl) reference electrode. SEM (TESCAN, Vega III, Czech Republic) was used to characterize the C-SPE.

4.2. Chemicals and Reagents. CCrP was supplied by PioChem International LLC. Stock solutions of 1×10^{-2} M CCrP were freshly prepared in ultrapure water and then kept refrigerated at 4 °C. In addition, *o*-PD, $K_4[Fe(CN)_6]$, $K_3[Fe(CN)_6]$, and potassium chloride were purchased from Sigma-Aldrich, USA. Methanol (HPLC grade) was used for the precipitation of the plasma proteins. Ultrapure water was used for the extraction of CCrP from plasma and CCrP removal from the MIP. Human plasma was purchased from the Holding Company for Biological Products and Vaccines (VACSERA, Egypt).

4.3. Electrochemical Polymerization of Poly(*o*-phenylenediamine). C-SPE was immersed in a 0.01 M solution of the template (CCrP), 0.01 M *o*-PD, and phosphate buffer (pH 7.0). The mixture was purged with N_2 for 15 min before starting the polymerization and throughout the polymerization process. Electropolymerization was accomplished by CV in the potential range of 0.0−0.9 V versus Ag/AgCl reference electrode, with a scan rate of 50 mV/s for 20 cycles. A C-SPE nonimprinted electrode (C-SPE/NIP) was prepared for use as a control. The preparation of C-SPE/NIP was performed using a similar procedure to C-SPE/MIP, except in the absence of the template. Then, the developed electrode was activated by washing to remove the CCrP with water under stirring; the targeted template was extracted from the polymer by continuous extraction for 30 min. The removal of the template was confirmed by EIS. Finally, the C-SPE-modified electrode was rinsed and then dried in a stream of N_2 to prepare it for CCrP analysis.

4.4. Physical and Electrochemical Characterization of the MIP. The surface morphology and film thickness of C-SPE/MIP and C-SPE/NIP samples were examined using SEM. CV characterization of the developed electrodes was performed in a phosphate buffer solution (pH 7.0) containing 10 mM $[Fe(CN)_6]/[Fe(CN)_6]^{3-/4-}$ (1:1) redox probe and 0.1 M KCl as a supporting electrolyte. Electropolymerization was performed using CV in the range of 0.0−0.8 V versus Ag/AgCl with a scan rate of 50 mV/s. EIS measurements were performed in the three-electrode configuration over the 0.1 Hz to 100 kHz frequency range, with a 5 mV alternating voltage signal and $[Fe[CN]_6]/[Fe[CN]_6]^{3-/4-}$ as the redox probe. The validity of the results was checked using Kramers−Kronig relations, then fitted to Randles' equivalent circuit using Nova 1.11.0 software to estimate the components.

4.5. Optimization of Experimental Conditions. To optimize sensor performance, the optimal electropolymerization conditions were carefully chosen, including the number of scan cycles, C-SPE/MIP incubation time in the sample solution, and pH of the background electrolyte.

4.6. Quantification of CCrP in Spiked Plasma. Human plasma samples were stored frozen and all analytical procedures were performed at room temperature. Aliquots of plasma (1.0 mL) were placed in Wasserman tubes and spiked with different volumes of standard CCrP solution. Plasma protein precipitation was performed by adding 3 mL of methanol/water (1:1) by vortex mixing. Then, the mixture was centrifuged with a speed of 5000 rpm for 15 min.[63] Aliquots of the supernatant were added to borate buffer with pH 8.5. The results were plotted as the capacitance change versus CCrP concentration for computing the corresponding regression equation in the linear range.

4.7. Bioanalytical Method Validation. The proposed bioanalytical method was developed and validated according to FDA guidelines for bioanalytical method validation.[64] The selectivity of the method was evaluated by testing different interference substances that are abundant in human plasma and are structural analogues to CCrP. The linearity of the proposed method was evaluated using five fortified plasma samples with CCrP concentrations in the range of 1×10^{-9} to 1×10^{-7} M at pH 8.5. The limit of quantification (LOQ) and limit of detection (LOD)[33] were calculated using $10S/X$ and $3S/X$ accordingly, where S is the standard deviation of the intercept of the regression line and X is the slope of the regression line. The accuracy and precision were determined at three concentration levels, QCL (1.0×10^{-9} mol/L), QCM (1.0×10^{-8} mol/L), and QCH (1.0×10^{-7} mol/L), as the average of three determinations and on 3 consecutive days.

https://doi.org/10.1021/acsomega.1c05098
ACS Omega 2021, 6, 31282−31291

The ME was evaluated by preparing CCrP solutions with concentrations QCL, QCM, and QCH: (i) **Set 1** was formulated in borate buffer (neat solvent); (ii) **Set 2** was formulated in extracted plasma; and (iii) **Set 3** was formulated in plasma. The capacitance of Sets 1, 2, and 3 were used to calculate the ME, RE, and PE values[65]

$$\text{ME}\ (\%) = \text{Set 2/Set 1} \times 100 \quad (1)$$

$$\text{RE}\ (\%) = \text{Set 3/Set 2} \times 100 \quad (2)$$

$$\text{PE}\ (\%) = \text{Set 3/Set 1} \times 100 \quad (3)$$

Different storage conditions were applied to evaluate the stability of the drugs in plasma, and the results were compared to the initial concentration. The following parameters were examined for the three prepared concentration levels (QCL, QCM, and QCH): (i) freeze−thaw stability following three freezing cycles and unassisted thawing at room temperature; and (ii) bench-top stability.

■ ASSOCIATED CONTENT

Supporting Information

The Supporting Information is available free of charge at https://pubs.acs.org/doi/10.1021/acsomega.1c05098.

Data of accuracy and precision for the determination of CCrP, cyclic voltammograms for the electropolymerization of *o*-PD, SEM images of C-SPE/NIP, Randles circuit, Nyquist plot of the C-SPE/NIP (as prepared/after washing/after exposure to the CCrP), UV spectroscopic study for (CCrP/*o*-PD/equimolar of *o*PD and CCrP), EIS experiment results with different CCrP concentrations, and chemical structure of (CCrP/Cr/CCr/CrP/ATP) (PDF)

■ AUTHOR INFORMATION

Corresponding Author

Amr M. Mahmoud − *Analytical Chemistry Department, Faculty of Pharmacy, Cairo University, Cairo 11562, Egypt;* orcid.org/0000-0002-7804-6442; Email: amr.bekhet@pharma.cu.edu.eg

Authors

Ibrahim F. Abo-Elmagd − *Bioanalysis Research Group, School of Pharmacy, Newgiza University, Giza 12256, Egypt;* orcid.org/0000-0002-9291-3055

Medhat A. Al-Ghobashy − *Bioanalysis Research Group, School of Pharmacy, Newgiza University, Giza 12256, Egypt; Analytical Chemistry Department, Faculty of Pharmacy, Cairo University, Cairo 11562, Egypt; Central Administration for Drug Control, Egyptian Drug Authority (EDA), Cairo 12654, Egypt;* orcid.org/0000-0002-3270-6804

Marianne Nebsen − *Analytical Chemistry Department, Faculty of Pharmacy, Cairo University, Cairo 11562, Egypt;* orcid.org/0000-0002-0687-2358

Nesrine S. El Sayed − *Department of Pharmacology and Toxicology, Faculty of Pharmacy, Cairo University, Cairo 11562, Egypt*

Shahira Nofal − *Department of Pharmacology and Toxicology, Faculty of Pharmacy, Helwan University, Helwan, Cairo 11795, Egypt*

Sameh H. Soror − *Department of Biochemistry and Molecular Biology, Faculty of Pharmacy and Center for Scientific Excellence, Helwan Structural Biology Research (HSBR), Faculty of Pharmacy, Helwan University, Helwan, Cairo 11795, Egypt*

Robert Todd − *ProChem International, LLC, Sheboygan, Wisconsin 53085-3325, United States*

Salwa A. Elgebaly − *Nour Heart, Inc., Vienna, Virginia 22180, United States; Faculty of Medicine, University of Connecticut, Farmington, Connecticut 06030, United States*

Complete contact information is available at: https://pubs.acs.org/10.1021/acsomega.1c05098

Notes

The authors declare no competing financial interest.

■ ACKNOWLEDGMENTS

The work was supported by a grant from the Academy of Scientific Research and Technology (ASRT), Ministry of Scientific Research, Egypt (Project ID: ASRT-Jesor 2371), and by a grant from Nour Heart, Inc., (Grant #20175).

■ LIST OF ABBREVIATIONS

CCrP, cyclocreatine phosphate; MIP, molecularly imprinted polymer; FDA, Food and Drug Administration; ODD, Orphan Drug Designation; CTD, creatine transporter deficiency; HPLC, high-performance liquid chromatography; ATP, adenosine triphosphate; *o*-PD, *ortho*-phenylenediamine; PoPD, poly-*ortho*-phenylenediamine; C-SPEs, carbon screen-printed electrodes; EIS, electrochemical impedance spectroscopy; CV, cyclic voltammetry; SEM, scanning electron microscopy; NIP, nonimprinted electrode; LOQ, limit of quantification; LOD, limit of detection; ME, matrix effect; RE, recovery efficiency; PE, process efficiency

■ REFERENCES

(1) Elgebaly, S. A.; Poston, R.; Todd, R.; Helmy, T.; Almaghraby, A. M.; Elbayoumi, T.; Kreutzer, D. L. Cyclocreatine protects against ischemic injury and enhances cardiac recovery during early reperfusion. *Expert Rev. Cardiovasc. Ther.* **2019**, *17*, 683−697.

(2) FDA Orphan Drug Designations and Approvals.

(3) Elgebaly, S. A.; Wei, Z.; Tyles, E.; Elkerm, A. F.; Houser, S. L.; Gillies, C.; Kaddurah-Daouk, R. Enhancement of the recovery of rat hearts after prolonged cold storage by cyclocreatine phosphate. *Transplantation* **1994**, *57*, 803−806.

(4) Gorshkov, K.; Wang, A. Q.; Sun, W.; Fisher, E.; Frigeni, M.; Singleton, M.; Thorne, N.; Class, B.; Huang, W.; Longo, N.; Do, M. T.; Ottinger, E. A.; Xu, X.; Zheng, W. Phosphocyclocreatine is the dominant form of cyclocreatine in control and creatine transporter deficiency patient fibroblasts. *Pharmacol. Res. Perspect.* **2019**, *7*, No. e00525.

(5) Tao, D.; Leister, W.; Huang, W.; Alimardanov, A.; LeClair, C. A. Facile high-performance liquid chromatography mass spectrometry method for analysis of Cyclocreatine and Phosphocyclocreatine in complex mixtures of amino acids. *J. Agric. Food Chem.* **2019**, *67*, 7190−7196.

(6) Ibrahim, F. A.; Al-Ghobashy, M. A.; Abd El-Rahman, M. K.; Abo-Elmagd, I. F. Optimization and in line potentiometric monitoring of enhanced photocatalytic degradation kinetics of gemifloxacin using TiO_2 nanoparticles/H_2O_2. *Environ. Sci. Pollut. Res.* **2017**, *24*, 23880−23892.

(7) Yola, M. L.; Eren, T.; Atar, N. A molecular imprinted voltammetric sensor based on carbon nitride nanotubes: application to determination of melamine. *J. Electrochem. Soc.* **2016**, *163*, B588.

(8) Iost, R. M.; da Silva, W. C.; Madurro, J. M.; Madurro, A. G. B.; Franco, L.; Ferreira, F. N. C. Electrochemical nano (bio) sensors:

advances, diagnosis and monitoring of diseases. *Front. Biosci.* **2011**, *3*, 663−689.
(9) Malitesta, C.; Mazzotta, E.; Picca, R. A.; Poma, A.; Chianella, I.; Piletsky, S. A. MIP sensors−the electrochemical approach. *Anal. Bioanal. Chem.* **2012**, *402*, 1827−1846.
(10) Yola, M. L.; Atar, N. Electrochemical detection of atrazine by platinum nanoparticles/carbon nitride nanotubes with molecularly imprinted polymer. *Ind. Eng. Chem. Res.* **2017**, *56*, 7631−7639.
(11) Viveiros, R.; Rebocho, S.; Casimiro, T. Green strategies for molecularly imprinted polymer development. *Polymers* **2018**, *10*, 306.
(12) Abd El-Rahman, M. K.; Mazzone, G.; Mahmoud, A. M.; Sicilia, E.; Shoeib, T. Novel Choline Selective Electrochemical Membrane Sensor with Application in Milk Powders and Infant Formulas. *Talanta* **2021**, *221*, 121409.
(13) Topcu, C.; Isildak, I. Novel Micro Flow Injection Analysis System for the Potentiometric Determination of Tetraborate Ions in Environmental Samples. *Anal. Lett.* **2021**, *54*, 854−866.
(14) Kröger, S.; Turner, A. P.; Mosbach, K.; Haupt, K. Imprinted polymer-based sensor system for herbicides using differential-pulse voltammetry on screen-printed electrodes. *Anal. Chem.* **1999**, *71*, 3698−3702.
(15) Ang, Q. Y.; Low, S. C. Feasibility study on molecularly imprinted assays for biomedical diagnostics. *Sens. Rev.* **2019**, *39*, 862.
(16) Levi, R.; McNiven, S.; Piletsky, S. A.; Cheong, S.-H.; Yano, K.; Karube, I. Optical detection of chloramphenicol using molecularly imprinted polymers. *Anal. Chem.* **1997**, *69*, 2017−2021.
(17) Schirhagl, R. Bioapplications for molecularly imprinted polymers. *Anal. Chem.* **2014**, *86*, 250−261.
(18) Attallah, O. A.; Al-Ghobashy, M. A.; Ayoub, A. T.; Nebsen, M. Magnetic molecularly imprinted polymer nanoparticles for simultaneous extraction and determination of 6-mercaptopurine and its active metabolite thioguanine in human plasma. *J. Chromatogr. A* **2018**, *1561*, 28−38.
(19) Andersson, L. I. Molecular imprinting for drug bioanalysis: A review on the application of imprinted polymers to solid-phase extraction and binding assay. *J. Chromatogr. B: Biomed. Sci. Appl.* **2000**, *739*, 163−173.
(20) Yola, M. L.; Göde, C.; Atar, N. Molecular imprinting polymer with polyoxometalate/carbon nitride nanotubes for electrochemical recognition of bilirubin. *Electrochim. Acta* **2017**, *246*, 135−140.
(21) Li, X.; He, Y.; Zhao, F.; Zhang, W.; Ye, Z. Molecularly imprinted polymer-based sensors for atrazine detection by electropolymerization of o-phenylenediamine. *RSC Adv.* **2015**, *5*, 56534−56540.
(22) Peng, Y.; Su, H. Recent innovations of molecularly imprinted electrochemical sensors based on electropolymerization technique. *Curr. Anal. Chem.* **2015**, *11*, 307−317.
(23) Gui, R.; Jin, H.; Guo, H.; Wang, Z. Recent advances and future prospects in molecularly imprinted polymers-based electrochemical biosensors. *Biosens. Bioelectron.* **2018**, *100*, 56−70.
(24) Kadirsoy, S.; Atar, N.; Yola, M. L. Molecularly imprinted QCM sensor based on delaminated MXene for chlorpyrifos detection and QCM sensor validation. *New J. Chem.* **2020**, *44*, 6524−6532.
(25) Özcan, N.; Medetalibeyoglu, H.; Akyıldırım, O.; Atar, N.; Yola, M. L. Electrochemical detection of amyloid-β protein by delaminated titanium carbide MXene/multi-walled carbon nanotubes composite with molecularly imprinted polymer. *Mater. Today Commun.* **2020**, *23*, 101097.
(26) Özcan, N.; Karaman, C.; Atar, N.; Karaman, O.; Yola, M. L. A novel molecularly imprinting biosensor including graphene quantum dots/multi-walled carbon nanotubes composite for interleukin-6 detection and electrochemical biosensor validation. *ECS J. Solid State Sci. Technol.* **2020**, *9*, 121010.
(27) Karimi-Maleh, H.; Yola, M. L.; Atar, N.; Orooji, Y.; Karimi, F.; Senthil Kumar, P.; Rouhi, J.; Baghayeri, M. A novel detection method for organophosphorus insecticide fenamiphos: Molecularly imprinted electrochemical sensor based on core-shell Co3O4@ MOF-74 nanocomposite. *J. Colloid Interface Sci.* **2021**, *592*, 174−185.
(28) Böke, C. P.; Karaman, O.; Medetalibeyoglu, H.; Karaman, C.; Atar, N.; Yola, M. L. A new approach for electrochemical detection of organochlorine compound lindane: Development of molecular imprinting polymer with polyoxometalate/carbon nitride nanotubes composite and validation. *Microchem. J.* **2020**, *157*, 105012.
(29) Mert, S.; Bankoğlu, B.; Özkan, A.; Atar, N.; Yola, M. L. Electrochemical sensing of ractopamine by carbon nitride nanotubes/ionic liquid nanohybrid in presence of other β-agonists. *J. Mol. Liq.* **2018**, *254*, 8−11.
(30) Mihailescu, C. M.; Stan, D.; Savin, M.; Moldovan, C. A.; Dinulescu, S.; Radulescu, C. H.; Firtat, B.; Muscalu, G.; Brasoveanu, C.; Ion, M.; Dragomir, D.; Stan, D.; Ion, A. C. Platform with biomimetic electrochemical sensors for adiponectin and leptin detection in human serum. *Talanta* **2020**, *210*, 120643.
(31) Couto, R. A. S.; Costa, S. S.; Mounssef, B., Jr; Pacheco, J. G.; Fernandes, E.; Carvalho, F.; Rodrigues, C. M. P.; Delerue-Matos, C.; Braga, A. A. C.; Moreira Gonçalves, L.; Quinaz, M. B. Electrochemical sensing of ecstasy with electropolymerized molecularly imprinted poly (o-phenylenediamine) polymer on the surface of disposable screen-printed carbon electrodes. *Sens. Actuators, B* **2019**, *290*, 378−386.
(32) Mazzotta, E.; Picca, R. A.; Malitesta, C.; Piletsky, S. A.; Piletska, E. V. Development of a sensor prepared by entrapment of MIP particles in electrosynthesised polymer films for electrochemical detection of ephedrine. *Biosens. Bioelectron.* **2008**, *23*, 1152−1156.
(33) Sharma, P. S.; Pietrzyk-Le, A.; D'Souza, F.; Kutner, W. Electrochemically synthesized polymers in molecular imprinting for chemical sensing. *Anal. Bioanal. Chem.* **2012**, *402*, 3177−3204.
(34) Pacheco, J. G.; Rebelo, P.; Cagide, F.; Gonçalves, L. M.; Borges, F.; Rodrigues, J. A.; Delerue-Matos, C. Electrochemical sensing of the thyroid hormone thyronamine (T0AM) via molecular imprinted polymers (MIPs). *Talanta* **2019**, *194*, 689−696.
(35) Camurri, G.; Ferrarini, P.; Giovanardi, R.; Benassi, R.; Fontanesi, C. Modelling of the initial stages of the electropolymerization mechanism of o-phenylenediamine. *J. Electroanal. Chem.* **2005**, *585*, 181−190.
(36) Ates, M. A review study of (bio) sensor systems based on conducting polymers. *Mater. Sci. Eng., C* **2013**, *33*, 1853−1859.
(37) Bilal, S.; Holze, R. Electrochemical copolymerization of o-toluidine and o-phenylenediamine. *J. Electroanal. Chem.* **2006**, *592*, 1−13.
(38) Kong, Y.; Shan, X.; Tao, Y.; Chen, Z.; Xue, H. Synthesis of Poly (o-phenylenediamine-co-o-aminophenol) via Electrochemical Copolymerization and its Electrical Properties. *J. Electrochem. Soc.* **2013**, *160*, G96−G101.
(39) Liu, X.; Li, C.; Wang, C.; Li, T.; Hu, S. The preparation of molecularly imprinted poly (o-phenylenediamine) membranes for the specific O, O-dimethyl-α-hydroxylphenyl phosphonate sensor and its characterization by AC impedance and cyclic voltammetry. *J. Appl. Polym. Sci.* **2006**, *101*, 2222−2227.
(40) Monti, P.; Bacciu, A.; Arrigo, P.; Marceddu, S.; Migheli, Q.; Serra, P. A.; Rocchitta, G. Chronoamperometry as effective alternative technique for electro-synthesis of ortho-phenylendiamine permselective films for biosensor applications. *J. Appl. Polym. Sci.* **2020**, *137*, 49172.
(41) Rajeshwari, V.; Mahalakshmi, B. Synthesis and Characterization of Nanosize Poly (p-phenylenediamine) in the presence of Benzalkonium Chloride. *Int. J. Adv. Sci. Res. Manag.* **2019**, No. Special Issue4, 94−99.
(42) Kutner, W.; Sharma, P. S. *Molecularly Imprinted Polymers for Analytical Chemistry Applications*; Royal Society of Chemistry, 2018; Vol. *28*.
(43) Andersson, L. I.; Mosbach, K. Enantiomeric resolution on molecularly imprinted polymers prepared with only non-covalent and non-ionic interactions. *J. Chromatogr. A* **1990**, *516*, 313−322.
(44) Mayes, A.; Whitcombe, M. Synthetic strategies for the generation of molecularly imprinted organic polymers. *Adv. Drug Deliv. Rev.* **2005**, *57*, 1742−1778.

https://doi.org/10.1021/acsomega.1c05098
ACS Omega 2021, 6, 31282−31291

(45) Norrlöw, O.; Glad, M.; Mosbach, K. Acrylic polymer preparations containing recognition sites obtained by imprinting with substrates. *J. Chromatogr. A* **1984**, *299*, 29−41.
(46) Ansell, R. Molecularly imprinted polymers for the enantioseparation of chiral drugs. *Adv. Drug Deliv. Rev.* **2005**, *57*, 1809−1835.
(47) Maier, N. M.; Lindner, W. Chiral recognition applications of molecularly imprinted polymers: a critical review. *Anal. Bioanal. Chem.* **2007**, *389*, 377−397.
(48) Tiwari, M. P.; Prasad, A. Molecularly imprinted polymer based enantioselective sensing devices: A review. *Anal. Chim. Acta* **2015**, *853*, 1−18.
(49) Malitesta, C.; Losito, I.; Zambonin, P. G. Molecularly imprinted electrosynthesized polymers: new materials for biomimetic sensors. *Anal. Chem.* **1999**, *71*, 1366−1370.
(50) Cheng, Z.; Wang, E.; Yang, X. Capacitive detection of glucose using molecularly imprinted polymers. *Biosens. Bioelectron.* **2001**, *16*, 179−185.
(51) Patolsky, F.; Filanovsky, B.; Katz, E.; Willner, I. Photoswitchable antigen− antibody interactions studied by impedance spectroscopy. *J. Phys. Chem. B* **1998**, *102*, 10359−10367.
(52) Feng, L.; Liu, Y.; Tan, Y.; Hu, J. Biosensor for the determination of sorbitol based on molecularly imprinted electrosynthesized polymers. *Biosens. Bioelectron.* **2004**, *19*, 1513−1519.
(53) Zhao, X.; Zhang, W.; Chen, H.; Chen, Y.; Huang, G. Disposable electrochemical ascorbic acid sensor based on molecularly imprinted poly (o-phenylenediamine)-modified dual channel screen-printed electrode for orange juice analysis. *Food Anal. Methods* **2014**, *7*, 1557−1563.
(54) Malitesta, C.; Palmisano, F.; Torsi, L.; Zambonin, P. G. Glucose fast-response amperometric sensor based on glucose oxidase immobilized in an electropolymerized poly (o-phenylenediamine) film. *Anal. Chem.* **1990**, *62*, 2735−2740.
(55) Mandell, D. J.; Chorny, I.; Groban, E. S.; Wong, S. E.; Levine, E.; Rapp, C. S.; Jacobson, M. P. Strengths of hydrogen bonds involving phosphorylated amino acid side chains. *J. Am. Chem. Soc.* **2007**, *129*, 820−827.
(56) Liu, Z.; Huang, S.; Jiang, D.; Liu, B.; Kong, J. A Novel Capacitive Immunosensor Using Electropolymerized Insulating Poly (o-phenylenediamine) Film on a Glass Carbon Electrode for Probing Transferrin. *Anal. Lett.* **2004**, *37*, 2283−2301.
(57) Losito, I.; Palmisano, F.; Zambonin, P. G. o-Phenylenediamine electropolymerization by cyclic voltammetry combined with electrospray ionization-ion trap mass spectrometry. *Anal. Chem.* **2003**, *75*, 4988−4995.
(58) Karimian, N.; Stortini, A. M.; Moretto, L. M.; Costantino, C.; Bogialli, S.; Ugo, P. Electrochemosensor for trace analysis of perfluorooctanesulfonate in water based on a molecularly imprinted poly (o-phenylenediamine) polymer. *ACS Sens.* **2018**, *3*, 1291−1298.
(59) Kan, X.; Liu, T.; Li, C.; Zhou, H.; Xing, Z.; Zhu, A. A novel electrochemical sensor based on molecularly imprinted polymers for caffeine recognition and detection. *J. Solid State Electrochem.* **2012**, *16*, 3207−3213.
(60) Ouyang, R.; Lei, J.; Ju, H.; Xue, Y. A molecularly imprinted copolymer designed for enantioselective recognition of glutamic acid. *Adv. Funct. Mater.* **2007**, *17*, 3223−3230.
(61) Chaocharoen, W.; Schulte, A.; Suginta, W. YKL-40 cancer biomarker electroanalysis in serum samples and model cell lysates: capacitive immunosensing compared with enzyme label immunosorbent assays (ELISA). *Analyst* **2017**, *142*, 503−510.
(62) Al-Ghobashy, M. A.; Kamal, S. M.; El-Sayed, G. M.; Attia, A. K.; Nagy, M.; ElZeiny, A.; Elrakaiby, M. T.; Nooh, M. M.; Abbassi, M.; Aziz, R. K. Determination of voriconazole and co-administered drugs in plasma of pediatric cancer patients using UPLC-MS/MS: A key step towards personalized therapeutics. *J. Chromatogr. B: Anal. Technol. Biomed. Life Sci.* **2018**, *1092*, 489−498.
(63) Wang, J.-m.; Chu, Y.; Li, W.; Wang, X.-y.; Guo, J.-h.; Yan, L.-l.; Ma, X.-h.; Ma, Y.-l.; Yin, Q.-h.; Liu, C.-x. Simultaneous determination of creatine phosphate, creatine and 12 nucleotides in rat heart by LC−MS/MS. *J. Chromatogr. B: Anal. Technol. Biomed. Life Sci.* **2014**, *958*, 96−101.
(64) FDA Bioanalytical Method Validation Guidance for Industry.
(65) Matuszewski, B. K.; Constanzer, M. L.; Chavez-Eng, C. M. Strategies for the assessment of matrix effect in quantitative bioanalytical methods based on HPLC− MS/MS. *Anal. Chem.* **2003**, *75*, 3019−3030.

https://doi.org/10.1021/acsomega.1c05098
ACS Omega 2021, 6, 31282−31291